

Controlling chaos to solutions with complex eigenvalues

Oh-Jong Kwon^{1,*} and Hoyun Lee^{2,†}

¹*Department of Science Education, Gongju National University of Education, Gongju 314-711, Republic of Korea*

²*Department of Physics, Chungnam National University, Daejeon 305-764, Republic of Korea*

(Received 14 February 2002; published 5 February 2003)

We derive formulas for parameter and variable perturbations to control chaos using linearized dynamics. They are available irrespective of the dimension of the system, the number of perturbed parameters or variables, and the kinds of eigenvalues of the linearized dynamics. We illustrate this using the two coupled Duffing oscillators and the two coupled standard maps.

DOI: 10.1103/PhysRevE.67.026201

PACS number(s): 05.45.Gg

In 1990, Ott, Grebogi, and Yorke (OGY) first succeeded in controlling chaos by applying a tiny parameter modulation to dissipative systems [1]. They derived a simple formula of small parameter modulation to stabilize the chaotic system to one of infinitely many unstable periodic orbits inherently embedded in the system's strange attractor. The OGY work turns the presence of chaos into an advantage. The OGY method has since attracted growing interest and has been applied in various fields of science [2–4].

Some works on the controlling chaos in cases where the eigenvalues of the linearized dynamics at some periodic orbit points are complex numbers [5–7] were proposed in 1993. Complex eigenvalues appear commonly in high-dimensional systems [5], in Hamiltonian systems [6], and when we use generalized Poincaré sections [7,8]. In dissipative and conservative systems, the complex eigenvalues of the linearized dynamics usually occur due to flow rotation and area conservation, respectively.

Some methods have been proposed so far to treat the cases of complex eigenvalues. However, all these methods are available generically only in cases where Poincaré maps are two-dimensional. The convergence of the minimal expected deviation method [5] and the modified pole placement method [9] has never been proved [8] in more than two-dimensional map systems. And the modified OGY method [6] and the singular-value decomposition method [7] use the so-called unstable direction that can be obtained using the algorithm in Ref. [10]. The algorithm gives only the maximally unstable direction, but all unstable directions are needed, in general, to control chaos in high-dimensional systems. In this paper, we propose formulas for parameter and variable perturbations to control chaos in high-dimensional systems when the linearized dynamics has complex eigenvalues at some orbit points of the target periodic orbit.

We consider a chaotic system whose the Poincaré maps are d dimensional. If we will apply a control algorithm N times a period of the target periodic orbit, N generalized Poincaré section Σ^n , $n=0, \dots, (N-1)$ and generalized Poincaré maps $\Phi^n: \Sigma^n \rightarrow \Sigma^{n+1}$ should be considered. The trajectory and the target periodic orbit intersect each of these surfaces at the coordinates z^n and z_F^n , respectively.

We first consider the case of perturbing K parameters simultaneously at each control station Σ^n . Then the difference vector $x^n \equiv z^n - z_F^n$ is mapped from Σ^n to Σ^{n+1} by

$$x^{n+1} = M^n x^n + g^n p^n, \quad (1)$$

where p^n is a K -dimensional vector representing the perturbation of the available parameters at Σ^n . The $d \times d$ matrix $M^n = D_z \Phi^n(z_F^n, p_0)$ represents the linearization of P^n around z_F^n , where p_0 is a vector of nominal values of system parameters at which the system is chaotic. The $d \times K$ matrix $g^n = D_p \Phi^n(z_F^n, p_0)$ approximates the dependence of the map P^n on the control parameters. It is natural that Eq. (1) is the case only when $\|x^n\| \ll 1$ and $\|p^n\| \ll 1$. Note that the periodic orbit points z_F^n , the Jacobian matrices M^n , and the dependence of the dynamics on the parameter perturbation g^n depend on the control step n , which has to be taken modulo N . Note also that x^{n+1} generally depends on the values of parameter perturbation at previous Poincaré sections if we use a time delay coordinate embedding technique [11]. However, if we use the state-plus-parameter system instead of the original one [12], the linearized dynamics has the same form as in Eq. (1) [13,14].

We require $x=0$ by control [15]. This requirement implies d equations and therefore d unknown variables are needed for the equations to be solved uniquely. As the d unknown variables, we take $P = (p^n p^{n+1} \dots p^{n+Q-1} p_1^{n+Q} p_2^{n+Q} \dots p_R^{n+Q})$, where p_i^n is the i th element of K -dimensional column vector p^n . Here, nonnegative integers Q and R are quotient and remainder satisfying $d = KQ + R$. In specific, we require that $x^{n+Q+1} = 0$ after $Q+1$ successive controls. The solution P of $x^{n+Q+1} = 0$ is given by

$$P = (A^{-1}C)x^n, \quad (2)$$

where the $d \times d$ matrix $A = (a^n : a^{n+1} : \dots : a^{n+Q-1} : a_1^{n+Q} : a_2^{n+Q} : \dots : a_R^{n+Q})$ and the $d \times d$ matrix $C = -\prod_{i=0}^Q M^{n+i}$ [16,17]. Here, the $d \times K$ matrix $a^m = (a_1^m : a_2^m : \dots : a_K^m)$, where the $d \times 1$ matrix $a_k^{n+i} = \prod_{j=i+1}^Q M^{n+j} g_k^{n+i}$ and the $d \times 1$ matrix $a_k^{n+Q} = g_k^{n+Q}$.

We next consider the case of perturbing K variables simultaneously at each control station. Then x^n is mapped from Σ^n to Σ^{n+1} by

$$x^{n+1} = M^n x^n + h^n v^n, \quad (3)$$

*Electronic address: kwon@pro.gjue.ac.kr

†Electronic address: hoyunlee@cnu.ac.kr

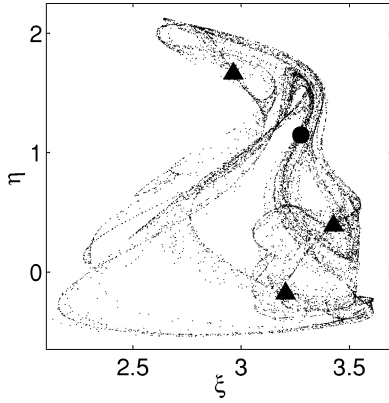


FIG. 1. The projection of the chaotic attractor of the two coupled Duffing oscillators into the ξ - η plane. As target periodic orbits, period-1 and period-3 orbits are represented by the solid circle and triangles, respectively. Here ξ and η have arbitrary units.

where the K -dimensional column vector v^n represents the perturbations of available variables at Σ^n and the $d \times K$ matrix $h^n = D_v \Phi^n(z_F^n, p_0)$ approximates the dependence of the map Φ^n on the control variables. The control requirement is the same as in the case of parameter perturbation discussed above. The d unknown variables of the equation $x^{n+Q+1} = 0$ are $V = (v^n v^{n+1} \dots v^{n+Q-1} v_1^{n+Q} v_2^{n+Q} \dots v_R^{n+Q})$, where v_i^n is the i th element of the K -dimensional column vector v^n . The solution V of $x^{n+Q+1} = 0$ is given by

$$V = (B^{-1}C)x^n, \quad (4)$$

where the $d \times d$ matrix $B = (b^n : b^{n+1} : \dots : b^{n+Q-1} : b_1^{n+Q} : b_2^{n+Q} : \dots : b_R^{n+Q})$. Here, the $d \times K$ matrix $b^n = (b_1^n : b_2^n : \dots : b_K^n)$ where the $d \times 1$ matrix $b_k^{n+Q} = h_k^{n+Q}$ and the $d \times 1$ matrix $b_k^{n+i} = \prod_{j=i+1}^Q M^{n+j} h_k^{n+i}$.

Note that there are no solutions in Eq. (2) and (4) if $\det(A) = 0$ and $\det(B) = 0$, respectively. This gives the controllability condition of our method. We also put a physically sensible restriction such that control is applied only when all elements of P or V are in between $-\delta$ and δ , a small number. Note that, at Σ^{n+Q} , P and V give the values of the first R available parameters and variables, respectively, but no information on the last $K - R$ ones, which are set zero.

To illustrate the availability of our formula (2) and (4), we control chaos in the two coupled Duffing oscillators [18] by perturbing two variables [19] simultaneously at multistations and next in the two coupled standard maps [20] by perturbing two parameters. The system of two coupled Duffing oscillators is described by $\ddot{\xi} + \alpha \dot{\xi} + \xi^3 = \eta + \beta \cos(\gamma t)$ and $\ddot{\eta} + \epsilon \dot{\eta} + \eta^3 = \xi$ [18]. Here t is time and dot over the variables ξ and η represents time derivative. The first oscillator is driven by an external periodic force, and the two oscillators interact with each other by ξ and η . When the parameters are fixed at $\alpha = 0.2, \beta = 10, \gamma = 1, \epsilon = 0.45$, the two coupled Duffing oscillators behave chaotically in the four-dimensional phase space. Figure 1 shows the projection of the chaotic attractor into ξ - η plane and, as target periodic orbits, period-1 and period-3 ones that are represented by a solid circle and solid upper triangles, respectively.

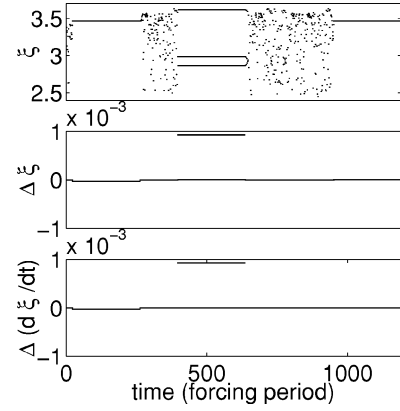


FIG. 2. The controlled trajectory and controlling variable perturbations of the two coupled Duffing oscillators, which is sampled at integer times of forcing period. $\Delta \xi$ and $\Delta(d\xi/dt)$ represent controlling perturbations of ξ and $\dot{\xi}$, respectively.

We will control chaos by perturbing two variables ξ and $\dot{\xi}$ simultaneously at each control station. Note that the chaos is controlled even if we perturb only one variable at each control station [12]. But the chaotic transient before stabilization is much longer than that of perturbing two variables simultaneously [21]. If we use N control stations, N Poincaré sections along the target periodic orbit are needed. We choose Poincaré sections $\Sigma^n (0 \leq n \leq N-1)$ with the phase of the external periodic force, $\theta^n = n(2\pi/N)$. M^n and h^n in Eq. (3) at each Σ^n are calculated numerically using the least square method [11]. In this example, $d = 4, K = 2, Q = 2, R = 0$. Thus, M^n, h^n, v^n in Eq. (3) are $4 \times 4, 4 \times 2, 2 \times 1$ matrices. The eigenvalues of M^n are usually complex numbers. For example, when $N = 1$, the eigenvalues of the period-1 orbit depicted by solid circle in Fig. 1 are $4.1191, -0.0596 + 0.1574i, -0.0596 - 0.1574i, 0.1441$.

Figure 2 shows the controlled trajectory when we use 50 control stations. Although we use 50 control stations, we sample the data only at the first Poincaré section θ^0 to present the result clearly. In this control, we set the maximum available variable perturbation δ to 5% of the range of the activity of ξ . That is, $\delta = 0.05 \times (3.6 - 2.1)$. The trajectory moves freely unless it comes into one of the controlling regions of the periodic orbit points in the Poincaré sections. As soon as it comes into the controlling region, we perturb the variables and the trajectory is stabilized to the target periodic orbit after two successive controls irrespective of the period of the target periodic orbit since $Q = 2$ and $R = 0$ in this example. In Fig. 2, the trajectory is initially chaotic and stabilized to the period-1 orbit and the control is maintained for 300 forcing periods. Next, we turn off the control to make the trajectory move freely. After some time, the trajectory comes into one of the controlling regions of the period-3 orbit. Just at that moment, we turn on the control and the trajectory is stabilized to the period-3 orbit after two successive controls. We maintain the control for 300 forcing periods. Last we cease the control to make the trajectory move freely. After some time, the trajectory comes into one of the

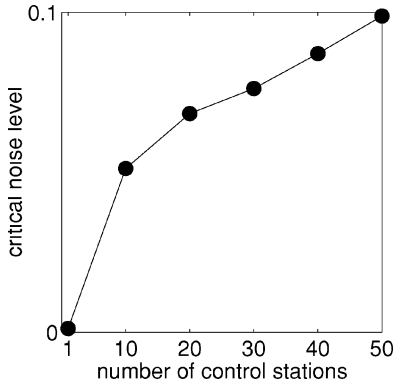


FIG. 3. Critical noise level for bursts to appear increases according to the number of control stations. Here the critical noise level is the maximum value of r in Eq. (5) at which initially stabilized trajectories experience no bursts in 1000 forcing periods.

controlling regions of the period-1 orbit. Then, we turn on the control and the trajectory is stabilized to the period-1 orbit again.

An advantage of controlling chaos using a number of control stations is that robustness of the control to noise increases exponentially [7]. The current state of the system can be measured only within an uncertainty due to noise. This error is magnified by a factor $\exp(\lambda_{\text{eff}}^n T)$ if we use only one control station. Here, λ_{eff}^n is the effective Lyapunov exponent of the target periodic orbit and T is its period. If we use N control stations, the error is magnified by a factor $\exp(\lambda_{\text{eff}}^n \Delta t)$ between Σ^n and Σ^{n+1} . Here $\Delta t = T/N$. Note that $\exp(\lambda_{\text{eff}}^n \Delta t)$ is the N -th root of $\exp(\lambda_{\text{eff}}^n T)$ in average. This means the influence of noise decreases exponentially according to the number of control stations.

To illustrate above discussion, we calculate the critical noise levels at which bursts start to appear at various numbers of control stations. The critical noise level is defined by the maximum at which an initially stabilized trajectory experiences no burst until it passes through 1000 forcing periods. Figure 3 shows the result when the noise has a normal distribution with mean zero and variance one. The horizontal and vertical axes represent the number of control stations and the corresponding critical noise level, respectively. In Fig. 3, we can easily see that the critical noise level and, thus, the robustness of the control to noise increases as the number of control stations increases. To obtain this result, we should solve the equations describing the two coupled Duffing oscillators under noise, which are stochastic differential equations. If we use the so-called Euler-Maruyama method [22], the stochastic differential equations are approximated by following difference equations:

$$w_{m+1} = w_m + hx_m + r\sqrt{h}\chi_m^w,$$

$$x_{m+1} = x_m + h[-\alpha x_m - w_m^4 + y_m + \beta \cos(mh)] + r\sqrt{h}\chi_m^x,$$

$$y_{m+1} = y_m + hx_m + r\sqrt{h}\chi_m^y,$$

$$z_{m+1} = z_m + h(-\epsilon z_m - y_m^3 + w_m) + r\sqrt{h}\chi_m^z, \quad (5)$$

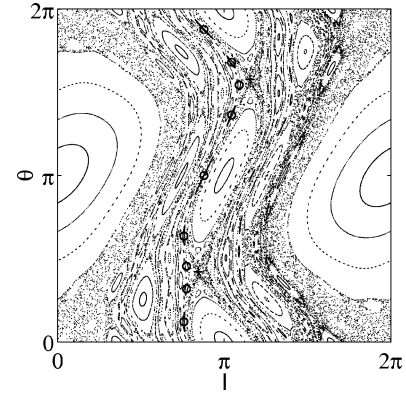


FIG. 4. The projection of the chaotic attractor of the two coupled standard maps into the I - θ plane. As target periodic orbits, period-2 unstable and period-9 elliptic periodic orbits are represented by plus signs and circles. Here, I and θ have arbitrary units.

where w_m , x_m , y_m , and z_m are the values of ξ , ξ , η , and $\dot{\eta}$ at $t = mh$, respectively. Here χ^w , χ^x , χ^y , and χ^z are random functions which are independent of each other, and the values are chosen from a normal distribution with mean zero and variance one. In our calculation we set $h = 10^{-5}$.

In order to illustrate the availability of our formula (2), we treat the two coupled standard maps [20]. Standard map is a typical Hamiltonian system. In Hamiltonian systems, the Jacobian of the linearized dynamics usually has complex eigenvalues due to the area conservation in the phase space. The two coupled standard maps are given by $I_{n+1} = I_n + K_I \sin \theta_n + \mu \sin(\theta_n + \phi_n)$, $\theta_{n+1} = \theta_n + I_{n+1}$, $J_{n+1} = J_n + K_J \sin \phi_n + \mu \sin(\theta_n + \phi_n)$, and $\phi_{n+1} = \phi_n + J_{n+1}$ [20]. Here

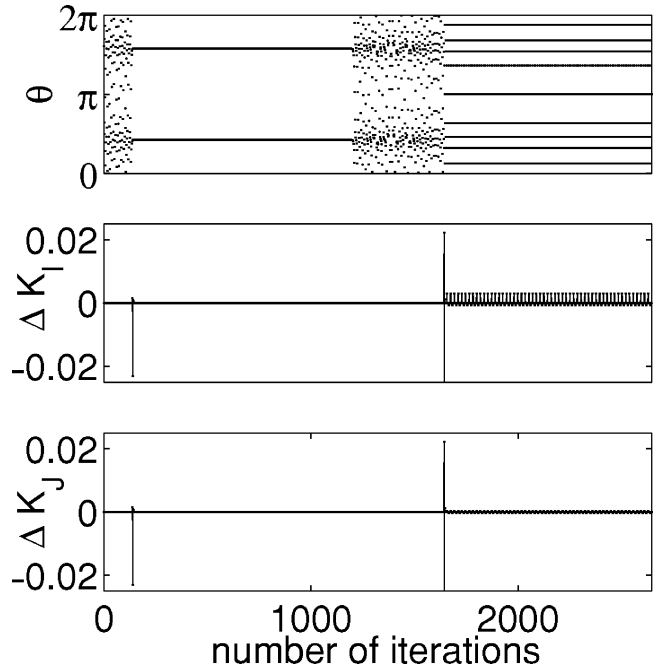


FIG. 5. The controlled trajectory and controlling parameter perturbations of the two coupled standard maps. ΔK_I and ΔK_J represent controlling perturbations of K_I and K_J , respectively. Chaotic transients are very long, in general.

both actions I, J and angles θ, ϕ are periodic, μ is the coupling constant. The one-dimensional Kolmogorov-Arnold-Moser (KAM) curves in the single standard map become two-dimensional KAM tori in the two coupled standard maps. Since a two-dimensional torus cannot divide a four-dimensional phase space, there can be the Arnold diffusion of particles around the KAM surfaces in the coupled maps.

When the parameters are fixed at $K_I=1, K_J=1, \mu=0.01$, the two coupled standard maps behave chaotically in the four-dimensional phase space. Figure 4 shows the projection of the chaotic attractor into $I-\theta$ plane and, as target periodic orbits, unstable period-2 and elliptic period-9 ones represented by plus signs and circles, respectively. Note that all orbit points of the unstable period-2 orbit have the same positive real eigenvalues: 1.6266, 1.5979, 0.6258, 0.6148. On the other hand, three of nine orbit points of the elliptic period-9 orbit have complex eigenvalues.

We control chaos by perturbing two parameters K_I and K_J simultaneously at each iteration. Note that more than two parameters should be perturbed due to symmetry [23,24]. In this control, we set the maximum available parameter perturbation $\delta=0.03 \times K_I$. Only when the trajectory comes into the controlling region of a periodic orbit point, we perturb the parameters and it is stabilized to the target periodic orbit

after two successive controls irrespective of the period of the target periodic orbit since $Q=2$ and $R=0$ in this example. Figure 5 shows that the trajectory is initially chaotic and stabilized to the period-2 unstable orbit, and the control is maintained for 300 iterations. Next, we turn off the control to make the trajectory move freely. After some time, the trajectory come into one of the controlling regions of the period-9 elliptic orbit. Just at that moment, we turn on the control and the trajectory is stabilized to the period-9 elliptic orbit after two successive controls.

We note that the phase space shown in Fig. 4 has very complex structure divided by large numbers of KAM layers and the chaotic transients for most initial conditions are very long. Thus, a targeting technique is needed to control chaos practically. No targeting technique has been proposed, which are available in high-dimensional Hamiltonian systems.

In conclusion, we have derived formulas of parameter and variable perturbations to control chaos. These are available even when the linearized dynamics has complex eigenvalues in high-dimensional systems. They also admit multiparameter or multivariable perturbations. We have shown the availability of our formulas by controlling chaos in the two coupled Duffing oscillators by perturbing two variables simultaneously at multistations and in the two coupled standard maps by perturbing two parameters simultaneously.

-
- [1] E. Ott, C. Grebogi, and J.A. Yorke, Phys. Rev. Lett. **64**, 1196 (1990).
- [2] *Coping with Chaos*, edited by E. Ott, T. Sauer, and J. A. Yorke, (Wiley, New York, 1994).
- [3] G. Chen and X. Dong, *From Chaos to Order* (World Scientific, Singapore, 1998).
- [4] *Handbook of Chaos Control*, edited by H. G. Schuster (Wiley-VCH, Weinheim, 1999).
- [5] C. Reyl, L. Flepp, R. Badii, and E. Brun, Phys. Rev. E **47**, 267 (1993).
- [6] Y.-C. Lai, M. Ding, and C. Grebogi, Phys. Rev. E **47**, 86 (1993).
- [7] B. Hübinger, R. Doerner, and W. Martienssen, Z. Phys. B: Condens. Matter **90**, 103 (1993).
- [8] Z. Galias, Int. J. Bifurcation Chaos Appl. Sci. Eng. **5**, 281 (1995).
- [9] T. Ritz, A.S.Z. Schweinsberg, U. Dressler, R. Doerner, B. Hübinger, and W. Martienssen, Chaos, Solitons Fractals **8**, 1559 (1997).
- [10] Y.-C. Lai, C. Grebogi, J.A. Yorke, and I. Kan, Nonlinearity **6**, 1 (1993).
- [11] U. Dressler and G. Nitsche, Phys. Rev. Lett. **68**, 1 (1992).
- [12] F. Romeiras, C. Grebogi, E. Ott, and W.P. Dayawansa, Physica D **58**, 165 (1992).
- [13] P. So and E. Ott, Phys. Rev. E **51**, 2955 (1995).
- [14] M. Ding, W. Yang, V. In, W.L. Ditto, M.L. Spano, and B. Gluckman, Phys. Rev. E **53**, 4334 (1996).
- [15] V. Petrov, V. Gáspar, J. Masere, and K. Showalter, Nature (London) **361**, 240 (1993), our requirement is a direct high dimensional extension of Petrov, *et al.*
- [16] Suppose that a^1, a^2, \dots, a^d are $d \times 1$ vectors. $(a^1 : a^2)$ is defined by a $d \times 2$ matrix whose first column is a^1 and second is a^2 . Following this definition, $(a^1 : a^2 : \dots : a^d)$ is a $d \times d$ matrix.
- [17] $\prod_{i=0}^j M^{n+i} \equiv M^{n+j} M^{n+j-1} \dots M^n$.
- [18] D. Xu and S.R. Bishop, Phys. Lett. A **210**, 273 (1996).
- [19] S. Hayes, C. Grebogi, and E. Ott, Phys. Rev. Lett. **70**, 3031 (1993).
- [20] B.P. Wood, A.J. Lichtenberg, and M.A. Lieberman, Phys. Rev. A **42**, 5885 (1990).
- [21] E. Barreto and C. Grebogi, Phys. Rev. E **52**, 3553 (1995).
- [22] *Numerical Solution of SDE Through Computer Experiments*, edited by P. E. Kloeden, E. Platen, and H. Schurz, (Springer-Verlag, Berlin, 1994).
- [23] H.G. Schuster, E. Niebur, E.R. Hunt, G.A. Johnson, and M. Löcher, Phys. Rev. Lett. **76**, 400 (1996).
- [24] M. Löcher and E.R. Hunt, Phys. Rev. Lett. **79**, 63 (1997).